A Shift to Randomness of Brain Oscillations in People with Autism

Meng-Chuan Lai, Michael V. Lombardo, Bhismadev Chakrabarti, Susan A. Sadek, Greg Pasco, Sally J. Wheelwright, Edward T. Bullmore, Simon Baron-Cohen, MRC AIMS Consortium, and John Suckling

Background: Resting-state functional magnetic resonance imaging (fMRI) enables investigation of the intrinsic functional organization of the brain. Fractal parameters such as the Hurst exponent, *H*, describe the complexity of endogenous low-frequency fMRI time series on a continuum from random ($H = .5$) to ordered ($H = 1$). Shifts in fractal scaling of physiological time series have been associated with neurological and cardiac conditions.

Methods: Resting-state fMRI time series were recorded in 30 male adults with an autism spectrum condition (ASC) and 33 age- and IQ-matched male volunteers. The Hurst exponent was estimated in the wavelet domain and between-group differences were investigated at global and voxel level and in regions known to be involved in autism.

Results: Complex fractal scaling of fMRI time series was found in both groups but globally there was a significant shift to randomness in the ASC (mean $H = .758$, SD $= .045$) compared with neurotypical volunteers (mean $H = .788$, SD $= .047$). Between-group differences in *H*, which was always reduced in the ASC group, were seen in most regions previously reported to be involved in autism, including cortical midline structures, medial temporal structures, lateral temporal and parietal structures, insula, amygdala, basal ganglia, thalamus, and inferior frontal gyrus. Severity of autistic symptoms was negatively correlated with *H* in retrosplenial and right anterior insular cortex.

Conclusions: Autism is associated with a small but significant shift to randomness of endogenous brain oscillations. Complexity measures may provide physiological indicators for autism as they have done for other medical conditions.

Key Words: Autism, complexity, fractal, Hurst exponent, oscillations, resting state fMRI

Autism spectrum conditions (ASC) are characterized by impairments in social communicative development, alongside repetitive stereotyped behaviors and/or restricted interests. The proposed underpinning neurobiological mechanisms involve limbic system (1,2), mentalizing circuit (3,4), prenatal hormone (5), early brain overgrowth and structural abnormalities (6,7), cerebral minicolumnopathy (8), and aberrant neural connectivity (9–11) and synchronization (12,13). Atypicality in specific components of systems has also been demonstrated, for instance in the social brain (2,11), corticostriatal system (7), and the default network (14–16).

Here, we further investigate whether neural systems are dynamically atypical in people with ASC. Rather than measuring differences between ASC and control groups in terms of activation by an experimental task, we have measured differences in the complexity of endogenous, low-frequency neurophysiological processes, using functional magnetic resonance imaging (fMRI) in a resting state (17–19). Previous studies of autism using resting-state fMRI showed relatively lower functional connectivity within the default network (14–16) and right-dominant altered regional homogeneity (20). However, no prior studies have investigated autism-related change in the complexity of resting-state fMRI time series.

Fractal scaling parameters, such as the fractal dimension (FD), the spectral exponent, or the Hurst exponent (*H*), can be used to define where an irregular process in space or time is located on the continuum of processes from randomness to Euclidean order. For example, the geologically irregular coastline of Norway has an FD $\sim$ 1.52, on a scale where a straight line has an FD $= 1$ and the randomly occupied plane has an FD $= 2$. When similar measures are applied to physiological time series, changes in fractal scaling have been observed as a corollary of disease or aging in the human brain (17,21,22) and heart (23,24), suggesting that such metrics could serve as physiological indicators of medical conditions. Several studies of electrocardiographic time series have shown that healthy cardiac dynamics have fractal scaling indicative of high complexity processes, which become more regular in association with end-stage heart disease and to a lesser extent in normal aging (23–25). Fractal scaling has also been measured in brain electrophysiological (26,27) and fMRI time series (17,22,28). The Hurst exponent, which is simply related to the fractal dimension, FD $= 2 - H$, and is estimated by expectation maximization from a wavelet decomposition of the time series (18), of resting-state fMRI time series in healthy young adults is approximately $H \sim .7$ to .8, on a scale where random noise has an $H = .5$ and a Euclidean line has an $H = 1$ (17). Alzheimer's disease has been associated with a shift to higher *H* indicative of more regular/persistent dynamics (17). Smaller increases in *H* are associated with normal aging and a single dose of muscarinic receptor antagonist (22). To illustrate the time series properties captured by changes in *H*, Figure 1 illustrates two fMRI time series sampled from posterior cingulate cortex, with $H = .88$ and .57, as well as a random time series with $H = .5$. Further information regarding fractality and fractal parameters is provided in Supplement 1.

In this context, we measured the complexity of resting-state fMRI dynamics in the brains of 30 men with ASC and 33 age- and IQ-matched neurotypical men. We hypothesized that there would

From the Autism Research Centre (M-CL, MVL, BC, SAS, GP, SJW, SB-C) and Brain Mapping Unit (ETB, JS), Department of Psychiatry, University of Cambridge, Cambridge; and Centre for Integrative Neuroscience and Neurodynamics (BC), School of Psychology and Clinical Language Sciences, University of Reading, Reading, United Kingdom.

Address correspondence to Meng-Chuan Lai, M.D., University of Cambridge, Autism Research Centre, Department of Psychiatry, Douglas House, 18B, Trumpington Road, Cambridge CB2 8AH, United Kingdom; E-mail: mcl45@cam.ac.uk.

Received Feb 1, 2010; revised Jun 20, 2010; accepted Jun 26, 2010.

0006-3223/$36.00
doi:10.1016/j.biopsych.2010.06.027

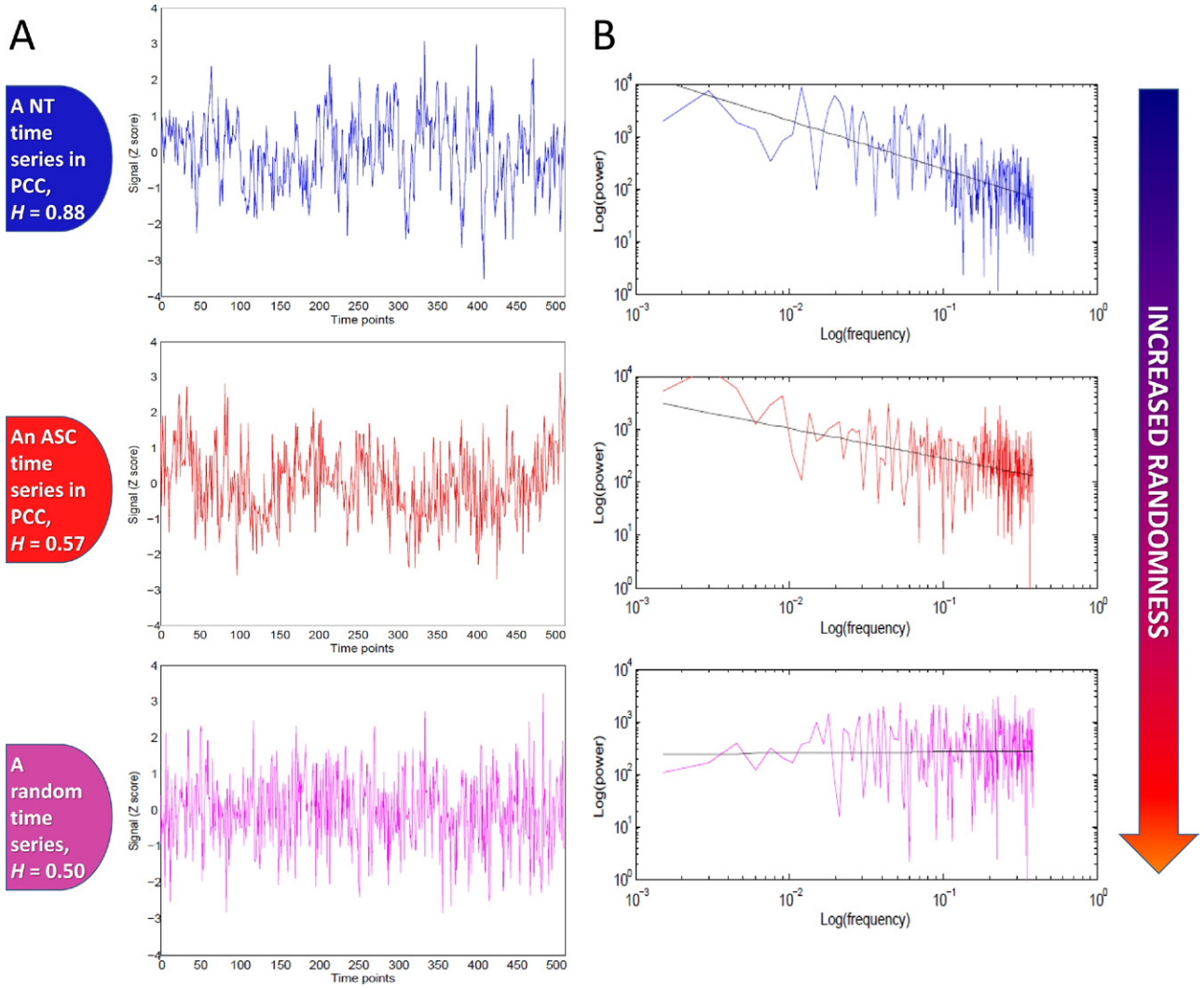

Figure 1. Illustrative functional magnetic resonance imaging (fMRI) and random time series demonstrating the concept of shift-to-randomness. Panel **(A)** shows normalized fMRI time series from a voxel in posterior cingulate cortex (Montreal Neurological Institute coordinate: −4, −36, 30) from a neurotypical (NT) (upper, blue, $H = .88$) and an autism spectrum condition (ASC) participant (middle, red, $H = .57$), as well as a simulated random (white Gaussian noise) time series (lower, purple, $H = .50$). Both fMRI time series exhibit self-similarity, but the one from the ASC participant shows less persistence, i.e., it is more similar to the random time series. Panel **(B)** illustrates the log-log plot of power spectrum for the three time series. For the NT time series, power attenuates as frequency increases (slope < 0); for the random time series, all frequencies are present with equal power in the spectrum (slope $= 0$); the ASC time series shows an intermediate slope between the NT and random time series, indicating a shift-to-randomness. *H*, Hurst exponent; PCC, posterior cingulate cortex.

be abnormalities of *H* in people with ASC, especially in brain regions known to be involved in autism.

Methods and Materials

Sample

Participants were recruited as part of the Medical Research Council Autism Imaging Multicentre Study. The inclusion criteria for the ASC group were being male, age ≥ 18 years, right-handed, normal or corrected vision, with English as first language, average intelligence (IQ ≥ 70), and a clinical diagnosis of autistic disorder or Asperger's syndrome based on DSM-IV (29) or ICD-10 criteria (30). Diagnoses of autism were confirmed for 30 ASC participants using the Autism Diagnostic Interview-Revised (ADI-R) (31). An additional three participants who scored 1 point below threshold on the repetitive behavior domain of the ADI-R were also included because they met Autism Diagnostic Observation Schedule (ADOS) (32) criteria for autism spectrum and were diagnosed by experienced clinicians.

Neurotypical (NT) volunteers were recruited through local advertisements and satisfied the same inclusion criteria as the ASC group, except that they did not have an ASC themselves or in their family history. Exclusion criteria for both groups included current or historical psychotic disorders, substance-use disorders, medical disorders associated with autism (e.g., tuberous sclerosis, fragile X syndrome), intellectual disability, epilepsy, hyperkinetic disorder, and Tourette syndrome. Six of the 33 ASC participants reported a history of antidepressant use, whereas none of the NT participants did. None of the ASC or NT participants received antipsychotic medication. Informed written consent was obtained for all participants in accord with procedures approved by the Suffolk Research Ethics Committee.

Data from 3 ASC participants were excluded (2 due to incomplete brain coverage during scanning and 1 due to neuroradio-

logical diagnosis of agenesis of corpus callosum), leaving 30 ASC participants for subsequent analysis (Table S1 in Supplement 1).

Behavioral Measures

Individuals with ASC were assessed using the Module 4 of ADOS (32) and the ADI-R interviews (31) with their parents. They also completed the Autism Spectrum Quotient (33), which measures autistic traits in the general population. All participants completed the Wechsler Abbreviated Scale of Intelligence (34) to assess full-scale, verbal, and performance IQ.

Resting-State fMRI Data Acquisition

Functional magnetic resonance imaging data were acquired using a 3T GE Signa scanner (General Electric Medical Systems, Milwaukee, Wisconsin) at the Magnetic Resonance Imaging and Spectroscopy Unit, University of Cambridge, United Kingdom. Participants were asked to lie quietly in the scanner awake with eyes closed for 13 minutes and 39 seconds during sequential acquisition of 625 whole-brain T2*-weighted echo planar image volumes with the following parameters: relaxation time = 1302 msec; echo time = 30 msec; flip angle = 70°; matrix size = 64 × 64; field of view = 24 cm; 22 anterior commissure-posterior commissure aligned slices per image volume; 4 mm axial slice thickness; 1 mm slice gap. The first 113 time points were discarded, leaving 512 (2^9) images analyzed by the discrete wavelet transform for estimation of the Hurst exponent (17).

Resting-State fMRI Data Preprocessing and Time Series Modeling

Following geometric motion correction, slice timing correction, and global image rescaling (35), volumes were spatially smoothed with a two-dimensional Gaussian kernel sized 4.4 mm full width at half maximum. The Hurst exponent was estimated at each intracerebral voxel using a maximum likelihood estimator in the wavelet domain (17,28) (see Supplement 1 for further information and Bullmore *et al.* [18] for introductory review of wavelet methods in fMRI.) This method models endogenous fMRI time series as a fractional Gaussian noise parameterized by its variance and Hurst exponent $0 < H < 1$: if $H = .5$, the process is a white Gaussian noise; if $0 < H < .5$, it is an antipersistent process; and if $.5 < H < 1$, it is a persistent, long-memory process with a $1/f$ power spectrum (Figure 1). Previous fMRI studies have shown that typically $H \sim .7$ to .8 with higher values in gray matter (GM) than in white matter (WM), and voxels with $H < .5$ tend to concentrate in cerebrospinal fluid (17). The motion-corrected image volumes and maps of H in each individual's native space were co-registered into the standard space of the Montreal Neurological Institute by applying the affine transformation parameters previously derived by registration of each individual's time-averaged fMRI data to the echo planar imaging template image (http://www.fil.ion.ucl.ac.uk/spm/). All preprocessing and time series analysis steps (including the estimation of H) were implemented using the CamBA software library (Brain Mapping Unit, University of Cambridge, Cambridge, United Kingdom), freely available for download at http://www-bmu.psychiatry.cam.ac.uk/software/.

Regional Parcellation

Each Hurst map was parcelled into a number of different regions by mapping the data onto three sets of regions-of-interest (ROIs) defined independently.

Regions Repeatedly Reported to be Structurally or Cerebrovascularly Abnormal in Autism. These were chosen from abnormal regions highlighted throughout the literature on structural magnetic resonance imaging and perfusion-weighted magnetic resonance imaging in ASC, including medial frontal structures (36–40), cingulate cortices (38,41–43), left pars opercularis (44,45), parietal structures (36,46–48), temporal structures (36–38,40,43,46,49–54), amygdala (2,7,55–57), insula (53,54,58), caudate (37,38,48,59–61), and thalamus (61–63) (Table S2 in Supplement 1). The cerebellum was not examined, as in some participants its most inferior part was not fully covered in the images. Several control regions reported to be intact in ASC were selected for comparison, including the primary sensory, motor, and visual cortices. These ROIs were created according to the Automatic Anatomical Labeling template (64).

Social Brain Regions Identified to be Consistently Underactivated in Previous fMRI Studies of Social Cognition in Autism. These were generated from a set of peak coordinates from quantitative meta-analyses of all fMRI studies of social task-activations reported to date on autism (Figure S3 and Table S3 in Supplement 1). They were selected from the peaks of hypoactivations (control subjects > ASC) across the entire social cognitive literature (65). For each peak coordinate, the ROI was constructed as a spherical binary mask 10 mm in diameter using the fslmaths utility in the FSL 4.1 software library (Analysis Group, FMRIB, Oxford, United Kingdom). Hyperactive regions (ASC > control subjects) were not examined due to ambiguity across the literature with regard to studies observing hyperactivations as either indicative of deficits (e.g., compensatory recruitment or increased neural effort) or strengths (e.g., increased ease of processing, heightened recruitment because of cognitive strengths) in ASC.

Nonsocial Brain Regions Identified to be Consistently Underactivated in Previous fMRI Studies of Nonsocial Cognition in Autism. These were generated by the same procedure as above (Figure S3 and Table S3 in Supplement 1). They were selected from the peaks of hypoactivations (control subjects > ASC) across the entire nonsocial cognitive literature (65).

Statistical Analysis

The main focus was tests of between-group difference in H at global, regional, and voxel scales. All voxel-level analyses were conducted within a gray matter mask to restrict comparisons to gray matter regions. We also tested (at voxel level) for correlations between H and measures of autistic symptom severity.

Between-Group Comparisons. Separate general linear models were regressed onto global, regional (defined by the ROIs), and voxel estimates of H, with group as the independent variable. The standardized regression parameter for group was tested for statistical significance by parametric and nonparametric procedures. For voxel statistics, we used a permutation test that adjusted the probability threshold for statistical significance of multiple comparisons by controlling the expected number of false-positive cluster-level tests to be less than one per map (equivalent $p = .0027$, two-tailed) (35,66,67).

Social Versus Nonsocial Regional Effects. A two-way analysis of variance model was fit to the average regional H statistics generated by the social/nonsocial ROIs, comprising main effects of group and social/nonsocial subsets and the group-by-regional subset interaction, indicating the extent to which group effects were differently expressed in social versus nonsocial ROIs.

Correlations with Measures of Autistic Symptom Severity. For this, we only analyzed data from the ASC group ($n = 30$). A general linear model was regressed to voxel estimates of H with autistic symptoms (including social interaction, communication, and repetitive/stereotyped behaviors scores in ADI-R, and social-communication and stereotyped behavior and restricted interest scores in ADOS) as the independent variable and global mean H as a covariate. We used the same permutation test as above and applied a less stringent critical value of three error

clusters per image (equivalent $p = .0059$, two-tailed). Mean *H* was extracted for each significant cluster for visual representation of the correlation to symptom scores, for which Pearson's correlation was calculated.

Voxel-level permutation tests were implemented by the CamBA software. Regional and global level analyses were conducted in SPSS 16.0 (SPSS, Inc., Chicaco, Illinois) using independent sample *t* tests and Pearson's correlation. Parametric tests were adopted, as all extracted *H* values from the ROIs were normally distributed, as evidenced by nonsignificance results in normality tests (i.e., Kolmogorov-Smirnov test).

Results

Demographics and Behavioral Characteristics

There were no significant group differences in age or intelligence. The ASC group scored significantly higher on the Autism Spectrum Quotient (33), consistent with their diagnosis (Table S1 in Supplement 1).

Group Comparison: Global and Voxel-Level

The global mean *H* was significantly lower [GM: $t(61) = 2.611$, $p = .011$; WM: $t(61) = 2.205$, $p = .031$] in the ASC (GM: .758, SD = .045; WM: .725, SD = .051) than the NT group (GM: .788, SD = .047; WM: .755, SD = .057). Meanwhile, there were no significant group differences on total brain volume (NT: 1257 cm^3, ASC: 1233 cm^3, $p = .082$) or GM (NT: 777 cm^3, ASC: 745 cm^3, $p = .063$) and WM (NT: 479 cm^3, ASC: 488 cm^3, $p = .113$) volumes. The group differences of mean *H* in GM and WM remained significant after controlling for GM and WM volumes, respectively (GM: $p = .017$, WM: $p = .033$). In the whole-brain voxel-level analysis, four distributed clusters showed significantly lower mean *H* in ASC group (Figure 2). They involved bilateral 1) cortical midline structures: medial prefrontal cortex (MPFC, Brodmann area [BA] 10), supplementary motor area (BA 6, 8), anterior cingulate cortex (BA 32, 33), dorsal cingulate cortex (BA 24), posterior cingulate cortex (BA 23, 29, 30, 31), precuneus (BA 7, 31), and lingual gyrus (BA 18); 2) medial temporal structures: hippocampus and parahippocampal and fusiform gyrus (BA 19, 20, 35, 36, 37); 3) lateral temporal and parietal structures: posterior superior temporal sulcus, temporoparietal junction, inferior parietal lobule (BA 39, 40), superior temporal gyrus (BA 22), and temporal pole (BA 38); 4) insula and amygdala; 5) basal ganglia; 6) thalamus; and 7) inferior frontal gyrus (BA 44, 45).

Group Comparison: Structurally and Cerebrovascularly Abnormal ROIs

We then proceeded to a hypothesis-driven investigation to test group differences in *H* in regions consistently reported to be atypical in ASC. On the anatomical ROIs (Table S2 in Supplement 1), 27 of the 31 candidate affected regions in ASC showed significantly lower *H* in ASC than in NT, with effect sizes ranging from .27 to .40 ($p < .032$, corrected by false discovery rate at $q < .05$). None of the control regions showed significant group differences, even at an uncorrected statistical threshold of $p = .05$.

Group Comparison: Functional Social and Nonsocial ROIs

We observed a significant group by ROI set interaction [$F(1,61) = 5.309$, $p = .025$] and that the ASC participants showed significantly lower *H* than neurotypicals in the social [mean *H* for NT = .783, (SD = .044), ASC = .752, (SD = .045); $t(61) = 2.751$, $p = .008$] but not the nonsocial ROIs [mean *H* for NT = .792, (SD = .053), ASC = .776,

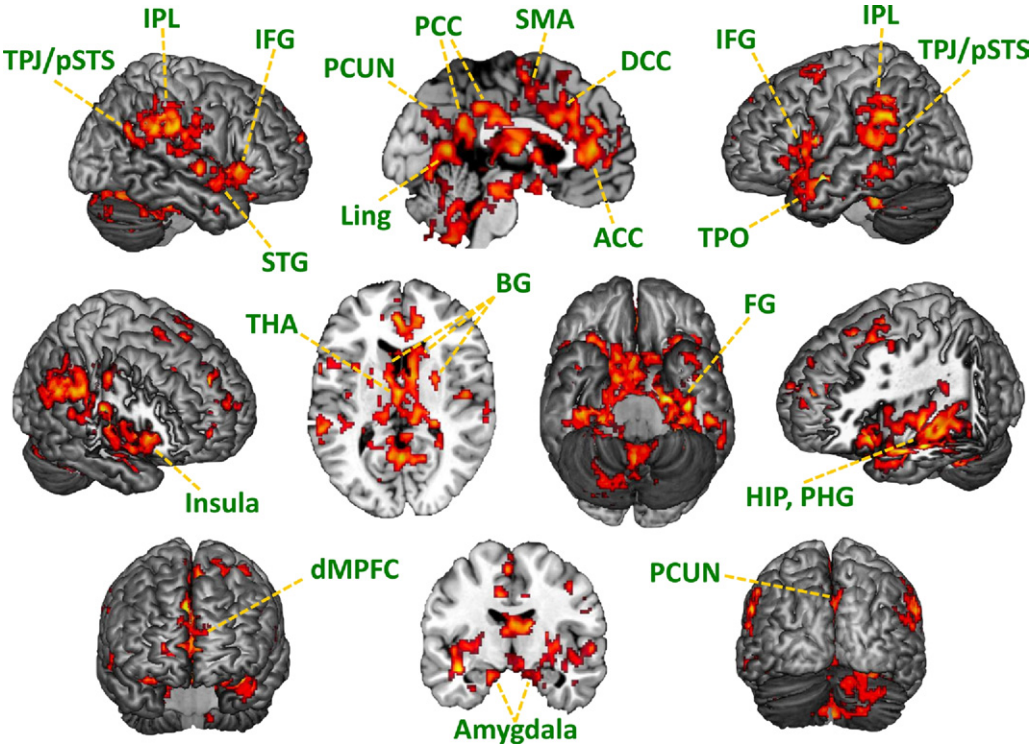

Figure 2. Whole-brain between-group differences in the Hurst exponent. Regions identified in voxel-level whole-brain analysis all showed significantly reduced values of *H* in autism spectrum condition brains in distributed clusters but with specific patterns. ACC, anterior cingulate cortex; BG, basal ganglia; DCC, dorsal cingulate cortex; dMPFC, dorsal medial prefrontal cortex; FG, fusiform gyrus; HIP, hippocampus; IFG, inferior frontal gyrus; IPL, inferior parietal lobule; Ling, lingual gyrus; PCC, posterior cingulate cortex; PCUN, precuneus; PHG, parahippocampal gyrus; pSTS, posterior superior temporal sulcus; SMA, supplementary motor area; STG, superior temporal gyrus; THA, thalamus; TPJ, temporoparietal junction; TPO, temporal pole.

(SD = .048); $t(61) = 1.219$, $p = .228$] (Figure S3 and Table S3 in Supplement 1).

Relationship Between *H* and Autistic Symptoms

The Hurst exponent was negatively correlated with ADI-R social scores in right anterior insula (peak Montreal Neurological Institute coordinate: 34, 8, 0; $r = -.60$, adjusted $R^2 = .26$; Figure S4A in Supplement 1). The ADOS social-communication scores were negatively correlated with *H* in bilateral retrosplenial cortices (peak Montreal Neurological Institute coordinate: 2, −58, 20; $r = -.57$, adjusted $R^2 = .21$; Figure S4B in Supplement 1). There were no clusters showing correlation in *H* with other symptom scores at the same statistical threshold. Mean *H* of the regions showing significant group differences (Figure 2) were not correlated with symptom scores.

Discussion

This study tested if differences in physiological complexity of the autistic versus neurotypical brain could be revealed by fractal analysis of resting-state fMRI time series. We confirmed that spontaneous blood oxygenation level-dependent (BOLD) signal fluctuations in the brain, specifically in regions implicated as atypical in previous autism neuroimaging studies, had lower Hurst exponents in the autism compared with neurotypical group, indicating a shift-to-randomness of brain oscillations in the autistic brain. Autistic symptom severity was also negatively correlated with *H* in several related regions. Here, we use shift-to-randomness in a purely descriptive, mathematical sense, with no value judgment attached. While we are aware some may interpret this pejoratively, we distance ourselves from such an interpretation, as *H* is not yet well understood in terms of its cognitive correlates.

Regional Dynamics Shifted Toward Randomness in ASC

Voxel-level analysis revealed lower *H* in bilateral cortical midline structures, medial temporal regions, lateral temporal-parietal and inferior frontal areas, and subcortical structures in ASC. These regions overlapped largely with the structurally implicated ROIs in a complementary hypothesis-driven analysis. At a functional level, lower *H* was also observed in ASC across regions that are consistently hypoactive during social tasks but not for regions hypoactive during nonsocial tasks. Most importantly, there were no group differences in areas where abnormalities had not been consistently reported, such as primary sensory, motor, and visual cortices. Thus, fractal analysis was effective in detecting atypical neural organization in regions previously reported atypical in autism, characterized by a shift of brain dynamics to randomness compared with the neurotypical brain. A shift-to-randomness in whole-brain network organization has recently been shown using a graph theory approach in schizophrenia (68) and Alzheimer's disease (69). Our findings have further demonstrated that changes in randomness of measurable neurophysiological signals are also seen in ASC, at the level of regional organization.

The regions appear to fall into three categories: social brain (70–72), connection hubs, and regions related to motor organization. Cortical midline structures (e.g., MPFC and cingulate) and the hippocampal formation form a neural circuit involved in self-projective/simulation processes (73) such as mentalizing, self-referential cognitive processing (74,75), autobiographical memory and prospection into the future (76), perspective taking (77), scene construction, and spatial navigation (78). Together with inferior parietal lobule they constitute the default network (79). Several studies implicate atypical dorsal MPFC recruitment in ASC for self-referential emotion (80) or mentalizing (81–83) and atypical ventral MPFC activity during self-representation in this sample (84). Relatively lower functional connectivity among these regions has been repeatedly observed in ASC (14–16). Lateral temporal regions, including posterior superior temporal sulcus/temporoparietal junction, superior temporal gyrus, and temporal pole, also serve as core components in the social brain and are integral for understanding movements, perspective taking, and convergence of social knowledge (71). Inferior frontal areas (BA 44), integral for language function and the mirror system (85), are also atypical in ASC (86). The insula and amygdala are critical for bottom-up automatic affective (70,87,88) and evaluative processing (89), empathy (90,91), and interoceptive awareness (92,93). Previous fMRI studies in ASC highlight hypoactive responses during face-processing and emotion tasks in the insula and amygdala (65). In summary, we suggest that the specificity with which more random brain dynamics affect these social brain components, whereas other neural circuits crucial for nonsocial cognitive processes are relatively unaffected, is not a coincidence. Social cognition likely relies on highly dynamic and coordinated information processing (94) and our observations of shift-to-randomness may be a critical physiological indicator for atypical social cognition in ASC. Certainly, some of these regions already show evidences of association with atypical social-communication function, in particular the right anterior insula and retrosplenial cortex (Figure S4 in Supplement 1); this right insula locus (34, 8, 0) is also close to the right insula region (34, 0, −2) showing significant correlation of anterior cingulate cortex-insula functional connectivity to social competence in healthy volunteers (95). However, these two areas are only part of a distributed set of regions showing more random signals in the autistic than the neurotypical brain, and average *H* in those other regions is not correlated with symptom scores. This indicates that signal randomness is correlated with symptoms only in very specific regions and that *H* should not be treated as a direct reflection of social-communication function.

Connection hubs have dense connections to the rest of the brain. The posterior cingulate cortex has been identified as the structural core of the cerebral cortex (96) and is also a major functional connector hub (97) associated with the default network (79). The thalamus is a sensory relay station characterized by extensive thalamocortical interconnections and the reciprocal nature of these neuronal loops (98,99). In the autistic brain, the thalamus has been shown atypical in its hyperconnectivity to the cerebral cortex (100), altered neurochemical composition (62) and relative size to total brain volume (63), and lower relative glucose metabolic rates (61). The more random signal in these regions in ASC may reflect perturbed information organization.

Finally, regions crucial for motor organization (supplementary motor area, basal ganglia, and possibly parts of cerebellum) also possessed more random signals in ASC. This may be relevant to the motor dysfunction in autism (101). However, more research is needed to assess whether this shift toward randomness has a bearing on network organization or atypical processing associated with these regions.

Physiological Meaning of *H*

The physiological meaning of *H* is obscured by our limited understanding at present on the relative contributions of neuronally and blood-supply mediated sources to the measured BOLD signal (102), as well as cardiac and respiratory signal confounds, and indeed the global signal. Nevertheless, we are willing to speculate that fractal scaling may serve as an indicator of the organization and coordination properties of the local neural circuits, although we are not able to delineate the relative contribution of each at this stage.

The shift-to-randomness may imply less coordinated signal organization at the local level of possibly small-scale neural circuits. Our preliminary analyses indicate that differences between pair-wise regional *H* are negatively correlated to their BOLD signal low-frequency correlation coefficients (Figure S5 in Supplement 1), suggesting a possible but complicated link between fractal scaling and functional connectivity, i.e., the more similar fractal scaling of the BOLD signals of a pair of regions (indicated by smaller difference in *H*), the higher their functional connectivity. Future correlation studies of fMRI fractal parameters with other regional measurements (e.g., gray matter density, local electromagnetic signal property, regional blood flow, or chemical composition) as well as functional connectivity may help illuminate their exact physiological significance.

The aging-related decrease of fractal dimension (increased *H*) depicted in previous studies (17,22) corresponds to the fractal theory of aging (103), in which hippocampal dynamics become less complex and more predictable. It is thus plausible that the lower *H* observed in the ASC relative to the NT brains reflects a reduction in aging-related decline in biological processes of the brain, given that recent studies showing brain maturation in adults with ASC might be atypical and delayed (104,105). We were not able to test this formally in the present study, given the insufficient sample size and relatively narrow age range of the participants. The physiological range of *H* for different brain structures, as well as their trajectories of change in the course of brain maturation, awaits further investigation. This may establish a clinical application for the Hurst exponent not currently available due to incomplete knowledge of the physiological processes that underpin its value, normal range, and sensitivity and specificity to different neuropsychiatric conditions.

Implications for the Neurobiology of Autism

Our findings have implications for theories of atypical connectivity (9,11) in ASC. The hypothesis of local (small-scale circuit) overconnectivity (9,11,106) has so far been supported by evidences of early brain overgrowth (6), cerebral cortical minicolumnopathy (8), and localized enlargement of cerebral radiate white matter (107). These perspectives argue that local structural abnormalities and disorganization result in local overconnectivity at the cost of decreased long-range information processing. The shift-to-randomness of BOLD signals in the implicated regions in the autistic brain may represent perturbed information processing within small-scale circuitry that may, in turn, have more profound effects on large-scale circuitry.

Limitations

Several caveats should be mentioned. First, inferences from fractal analysis are constrained by insufficient current knowledge of its exact physiological relation. This will become clearer with further research tying fractal parameters to other measurements. Second, because in some participants the most inferior part of cerebellum was not fully covered in the images, we were not able to make confident inferences about this important structure in autism neurobiology (7). Finally, because this study was limited to high-functioning male adults, it is unknown how the results may generalize to female subjects and individuals of other ages or intellectual levels. We are also agnostic about whether the observed changes in fractal dynamics are specific to ASC. Further clarity should become available when similar studies are conducted on other neuropsychiatric, especially neurodevelopmental conditions, such as intellectual disability, schizophrenia, or attention-deficit/hyperactivity disorder.

This research was conducted in association with the National Institute for Health Research, Collaborations for Leadership in Applied Health Research and Care for Cambridgeshire and Peterborough National Health Service Foundation Trust and the Medical Research Council Autism Imaging Multicentre Study Consortium (MRC AIMS Consortium). The MRC AIMS Consortium is a United Kingdom collaboration between the Institute of Psychiatry at King's College, London, and the Universities of Cambridge and Oxford. It is funded by the Medical Research Council United Kingdom and headed by the Institute of Psychiatry. The Consortium members are in alphabetical order: Bailey AJ, Baron-Cohen S, Bolton PF, Bullmore ET, Carrington S, Chakrabarti B, Daly EM, Deoni SC, Ecker C, Happé F, Henty J, Jezzard P, Johnston P, Jones DK, Lai M-C, Lombardo MV, Madden A, Mullins D, Murphy C, Murphy DGM, Pasco G, Sadek S, Spain D, Stewart R, Suckling J, Wheelwright S, and Williams SC.

We are grateful to the participants for taking part in this study.

Dr. Lai is supported by the Ministry of Education, Taiwan, and Girton College, University of Cambridge. Dr. Lombardo is supported by the Shirley Foundation and Cambridge Overseas Trust. Professor Bullmore is employed half-time as a professor in the Department of Psychiatry at the University of Cambridge and employed half-time by GlaxoSmithKline, plc. Professors Baron-Cohen and Suckling are supported by the Medical Research Council United Kingdom. Drs. Pasco and Chakrabarti and Ms. Wheelwright and Sadek reported no biomedical financial interests or potential conflicts of interest.

Supplementary material cited in this article is available online.

1. Bauman ML, Kemper TL (2005): Neuroanatomic observations of the brain in autism: A review and future directions. *Int J Dev Neurosci* 23:183–187.
2. Baron-Cohen S, Ring HA, Bullmore ET, Wheelwright S, Ashwin C, Williams SC (2000): The amygdala theory of autism. *Neurosci Biobehav Rev* 24:355–364.
3. Frith U (2001): Mind blindness and the brain in autism. *Neuron* 32:969–979.
4. Baron-Cohen S, Ring H, Moriarty J, Schmitz B, Costa D, Ell P (1994): Recognition of mental state terms. Clinical findings in children with autism and a functional neuroimaging study of normal adults. *Br J Psychiatry* 165:640–649.
5. Baron-Cohen S (2002): The extreme male brain theory of autism. *Trends Cogn Sci* 6:248–254.
6. Courchesne E, Pierce K, Schumann CM, Redcay E, Buckwalter JA, Kennedy DP, Morgan J (2007): Mapping early brain development in autism. *Neuron* 56:399–413.
7. Amaral DG, Schumann CM, Nordahl CW (2008): Neuroanatomy of autism. *Trends Neurosci* 31:137–145.
8. Casanova MF, van Kooten IA, Switala AE, van Engeland H, Heinsen H, Steinbusch HW, *et al.* (2006): Minicolumnar abnormalities in autism. *Acta Neuropathol* 112:287–303.
9. Belmonte MK, Allen G, Beckel-Mitchener A, Boulanger LM, Carper RA, Webb SJ (2004): Autism and abnormal development of brain connectivity. *J Neurosci* 24:9228–9231.
10. Just MA, Cherkassky VL, Keller TA, Minshew NJ (2004): Cortical activation and synchronization during sentence comprehension in high-functioning autism: Evidence of underconnectivity. *Brain* 127:1811–1821.
11. Baron-Cohen S, Belmonte MK (2005): Autism: A window onto the development of the social and the analytic brain. *Annu Rev Neurosci* 28:109–126.
12. Brock J, Brown CC, Boucher J, Rippon G (2002): The temporal binding deficit hypothesis of autism. *Dev Psychopathol* 14:209–224.
13. Uhlhaas PJ, Singer W (2006): Neural synchrony in brain disorders: Relevance for cognitive dysfunctions and pathophysiology. *Neuron* 52: 155–168.
14. Monk CS, Peltier SJ, Wiggins JL, Weng SJ, Carrasco M, Risi S, Lord C (2009): Abnormalities of intrinsic functional connectivity in autism spectrum disorders. *Neuroimage* 47:764–772.
15. Kennedy DP, Courchesne E (2008): The intrinsic functional organization of the brain is altered in autism. *Neuroimage* 39:1877–1885.
16. Weng SJ, Wiggins JL, Peltier SJ, Carrasco M, Risi S, Lord C, Monk CS (2010): Alterations of resting state functional connectivity in the de-

fault network in adolescents with autism spectrum disorders. *Brain Res* 1313:202–214.
17. Maxim V, Sendur L, Fadili J, Suckling J, Gould R, Howard R, Bullmore E (2005): Fractional Gaussian noise, functional MRI and Alzheimer's disease. *Neuroimage* 25:141–158.
18. Bullmore E, Fadili J, Maxim V, Sendur L, Whitcher B, Suckling J, *et al.* (2004): Wavelets and functional magnetic resonance imaging of the human brain. *Neuroimage* 23(suppl 1):S234–S249.
19. Bullmore E, Barnes A, Bassett DS, Fornito A, Kitzbichler M, Meunier D, Suckling J (2009): Generic aspects of complexity in brain imaging data and other biological systems. *Neuroimage* 47:1125–1134.
20. Paakki JJ, Rahko J, Long X, Moilanen I, Tervonen O, Nikkinen J, *et al.* (2010): Alterations in regional homogeneity of resting-state brain activity in autism spectrum disorders. *Brain Res* 1321:169–179.
21. Rasouli G, Rasouli M, Lenz FA, Verhagen L, Borrett DS, Kwan HC (2006): Fractal characteristics of human parkinsonian neuronal spike trains. *Neuroscience* 139:1153–1158.
22. Wink AM, Bernard F, Salvador R, Bullmore E, Suckling J (2006): Age and cholinergic effects on hemodynamics and functional coherence of human hippocampus. *Neurobiol Aging* 27:1395–1404.
23. Beckers F, Verheyden B, Couckuyt K, Aubert AE (2006): Fractal dimension in health and heart failure. *Biomed Tech (Berl)* 51:194–197.
24. Lin LY, Lin JL, Du CC, Lai LP, Tseng YZ, Huang SK (2001): Reversal of deteriorated fractal behavior of heart rate variability by beta-blocker therapy in patients with advanced congestive heart failure. *J Cardiovasc Electrophysiol* 12:26–32.
25. Beckers F, Verheyden B, Aubert AE (2006): Aging and nonlinear heart rate control in a healthy population. *Am J Physiol Heart Circ Physiol* 290:H2560–H2570.
26. Bullmore ET, Brammer MJ, Bourlon P, Alarcon G, Polkey CE, Elwes R, Binnie CD (1994): Fractal analysis of electroencephalographic signals intracerebrally recorded during 35 epileptic seizures: Evaluation of a new method for synoptic visualisation of ictal events. *Electroencephalogr Clin Neurophysiol* 91:337–345.
27. Linkenkaer-Hansen K, Nikouline VV, Palva JM, Ilmoniemi RJ (2001): Long-range temporal correlations and scaling behavior in human brain oscillations. *J Neurosci* 21:1370–1377.
28. Wink AM, Bullmore E, Barnes A, Bernard F, Suckling J (2008): Monofractal and multifractal dynamics of low frequency endogenous brain oscillations in functional MRI. *Hum Brain Mapp* 29:791–801.
29. American Psychiatric Association (2000): *Diagnostic and Statistical Manual of Mental Disorders, 4th ed, Text Revision*. Washington, DC: American Psychiatric Publishing.
30. World Health Organization (1992): *The ICD-10 Classification of Mental and Behavioural Disorders: Clinical Descriptions and Diagnostic Guidelines*. Geneva: World Health Organization.
31. Lord C, Rutter M, Le Couteur A (1994): Autism Diagnostic Interview-Revised: A revised version of a diagnostic interview for caregivers of individuals with possible pervasive developmental disorders. *J Autism Dev Disord* 24:659–685.
32. Lord C, Risi S, Lambrecht L, Cook EH Jr, Leventhal BL, DiLavore PC, *et al.* (2000): The autism diagnostic observation schedule-generic: A standard measure of social and communication deficits associated with the spectrum of autism. *J Autism Dev Disord* 30:205–223.
33. Baron-Cohen S, Wheelwright S, Skinner R, Martin J, Clubley E (2001): The autism-spectrum quotient (AQ): Evidence from Asperger syndrome/high-functioning autism, males and females, scientists and mathematicians. *J Autism Dev Disord* 31:5–17.
34. Wechsler D (1999): *Wechsler Abbreviated Scale of Intelligence (WASI)*. New York: The Psychological Corporation.
35. Suckling J, Davis MH, Ooi C, Wink AM, Fadili J, Salvador R, *et al.* (2006): Permutation testing of orthogonal factorial effects in a language-processing experiment using fMRI. *Hum Brain Mapp* 27:425–433.
36. Ke X, Hong S, Tang T, Zou B, Li H, Hang Y, *et al.* (2008): Voxel-based morphometry study on brain structure in children with high-functioning autism. *Neuroreport* 19:921–925.
37. Rojas DC, Peterson E, Winterrowd E, Reite ML, Rogers SJ, Tregellas JR (2006): Regional gray matter volumetric changes in autism associated with social and repetitive behavior symptoms. *BMC Psychiatry* 6:56.
38. McAlonan GM, Cheung V, Cheung C, Suckling J, Lam GY, Tai KS, *et al.* (2005): Mapping the brain in autism. A voxel-based MRI study of volumetric differences and intercorrelations in autism. *Brain* 128:268–276.
39. Abell F, Krams M, Ashburner J, Passingham R, Friston K, Frackowiak R, *et al.* (1999): The neuroanatomy of autism: A voxel-based whole brain analysis of structural scans. *Neuroreport* 10:1647–1651.
40. Waiter GD, Williams JH, Murray AD, Gilchrist A, Perrett DI, Whiten A (2004): A voxel-based investigation of brain structure in male adolescents with autistic spectrum disorder. *Neuroimage* 22:619–625.
41. Thakkar KN, Polli FE, Joseph RM, Tuch DS, Hadjikhani N, Barton JJ, Manoach DS (2008): Response monitoring, repetitive behaviour and anterior cingulate abnormalities in autism spectrum disorders (ASD). *Brain* 131:2464–2478.
42. Haznedar MM, Buchsbaum MS, Metzger M, Solimando A, Spiegel-Cohen J, Hollander E (1997): Anterior cingulate gyrus volume and glucose metabolism in autistic disorder. *Am J Psychiatry* 154:1047–1050.
43. Kwon H, Ow AW, Pedatella KE, Lotspeich LJ, Reiss AL (2004): Voxel-based morphometry elucidates structural neuroanatomy of high-functioning autism and Asperger syndrome. *Dev Med Child Neurol* 46: 760–764.
44. Nordahl CW, Dierker D, Mostafavi I, Schumann CM, Rivera SM, Amaral DG, Van Essen DC (2007): Cortical folding abnormalities in autism revealed by surface-based morphometry. *J Neurosci* 27:11725–11735.
45. Hadjikhani N, Joseph RM, Snyder J, Tager-Flusberg H (2006): Anatomical differences in the mirror neuron system and social cognition network in autism. *Cereb Cortex* 16:1276–1282.
46. Brieber S, Neufang S, Bruning N, Kamp-Becker I, Remschmidt H, Herpertz-Dahlmann B, *et al.* (2007): Structural brain abnormalities in adolescents with autism spectrum disorder and patients with attention deficit/hyperactivity disorder. *J Child Psychol Psychiatry* 48:1251–1258.
47. Ryu YH, Lee JD, Yoon PH, Kim DI, Lee HB, Shin YJ (1999): Perfusion impairments in infantile autism on technetium-99m ethyl cysteinate dimer brain single-photon emission tomography: Comparison with findings on magnetic resonance imaging. *Eur J Nucl Med* 26:253–259.
48. McAlonan GM, Suckling J, Wong N, Cheung V, Lienenkaemper N, Cheung C, Chua SE (2008): Distinct patterns of grey matter abnormality in high-functioning autism and Asperger's syndrome. *J Child Psychol Psychiatry* 49:1287–1295.
49. Neeley ES, Bigler ED, Krasny L, Ozonoff S, McMahon W, Lainhart JE (2007): Quantitative temporal lobe differences: Autism distinguished from controls using classification and regression tree analysis. *Brain Dev* 29:389–399.
50. Gendry Meresse I, Zilbovicius M, Boddaert N, Robel L, Philippe A, Sfaello I, *et al.* (2005): Autism severity and temporal lobe functional abnormalities. *Ann Neurol* 58:466–469.
51. Zilbovicius M, Boddaert N, Belin P, Poline JB, Remy P, Mangin JF, *et al.* (2000): Temporal lobe dysfunction in childhood autism: A PET study. Positron emission tomography. *Am J Psychiatry* 157:1988–1993.
52. Salmond CH, Ashburner J, Connelly A, Friston KJ, Gadian DG, Vargha-Khadem F (2005): The role of the medial temporal lobe in autistic spectrum disorders. *Eur J Neurosci* 22:764–772.
53. Salmond CH, Vargha-Khadem F, Gadian DG, de Haan M, Baldeweg T (2007): Heterogeneity in the patterns of neural abnormality in autistic spectrum disorders: Evidence from ERP and MRI. *Cortex* 43:686–699.
54. Ohnishi T, Matsuda H, Hashimoto T, Kunihiro T, Nishikawa M, Uema T, Sasaki M (2000): Abnormal regional cerebral blood flow in childhood autism. *Brain* 123:1838–1844.
55. Munson J, Dawson G, Abbott R, Faja S, Webb SJ, Friedman SD, *et al.* (2006): Amygdalar volume and behavioral development in autism. *Arch Gen Psychiatry* 63:686–693.
56. Schumann CM, Hamstra J, Goodlin-Jones BL, Lotspeich LJ, Kwon H, Buonocore MH, *et al.* (2004): The amygdala is enlarged in children but not adolescents with autism; the hippocampus is enlarged at all ages. *J Neurosci* 24:6392–6401.
57. Mosconi MW, Cody-Hazlett H, Poe MD, Gerig G, Gimpel-Smith R, Piven J (2009): Longitudinal study of amygdala volume and joint attention in 2- to 4-year-old children with autism. *Arch Gen Psychiatry* 66:509–516.
58. Hadjikhani N, Joseph RM, Manoach DS, Naik P, Snyder J, Dominick K, *et al.* (2009): Body expressions of emotion do not trigger fear contagion in autism spectrum disorder. *Soc Cogn Affect Neurosci* 4:70–78.
59. Stanfield AC, McIntosh AM, Spencer MD, Philip R, Gaur S, Lawrie SM (2008): Towards a neuroanatomy of autism: A systematic review and meta-analysis of structural magnetic resonance imaging studies. *Eur Psychiatry* 23:289–299.

60. Hollander E, Anagnostou E, Chaplin W, Esposito K, Haznedar MM, Licalzi E, *et al.* (2005): Striatal volume on magnetic resonance imaging and repetitive behaviors in autism. *Biol Psychiatry* 58:226–232.
61. Haznedar MM, Buchsbaum MS, Hazlett EA, Licalzi EM, Cartwright C, Hollander E (2006): Volumetric analysis and three-dimensional glucose metabolic mapping of the striatum and thalamus in patients with autism spectrum disorders. *Am J Psychiatry* 163:1252–1263.
62. Hardan AY, Minshew NJ, Melhem NM, Srihari S, Jo B, Bansal R, *et al.* (2008): An MRI and proton spectroscopy study of the thalamus in children with autism. *Psychiatry Res* 163:97–105.
63. Hardan AY, Girgis RR, Adams J, Gilbert AR, Keshavan MS, Minshew NJ (2006): Abnormal brain size effect on the thalamus in autism. *Psychiatry Res* 147:145–151.
64. Tzourio-Mazoyer N, Landeau B, Papathanassiou D, Crivello F, Etard O, Delcroix N, *et al.* (2002): Automated anatomical labeling of activations in SPM using a macroscopic anatomical parcellation of the MNI MRI single-subject brain. *Neuroimage* 15:273–289.
65. Lombardo MV, Baron-Cohen S, Belmonte MK, Chakrabarti B (in press): Neural endophenotypes for social behaviour in autism spectrum conditions. In: Decety J, Cacioppo J, editors. *Handbook of Social Neuroscience*. Oxford, UK: Oxford University Press.
66. Bullmore ET, Suckling J, Overmeyer S, Rabe-Hesketh S, Taylor E, Brammer MJ (1999): Global, voxel, and cluster tests, by theory and permutation, for a difference between two groups of structural MR images of the brain. *IEEE Trans Med Imaging* 18:32–42.
67. Suckling J, Bullmore E (2004): Permutation tests for factorially designed neuroimaging experiments. *Hum Brain Mapp* 22:193–205.
68. Rubinov M, Knock SA, Stam CJ, Micheloyannis S, Harris AW, Williams LM, Breakspear M (2009): Small-world properties of nonlinear brain activity in schizophrenia. *Hum Brain Mapp* 30:403–416.
69. Stam CJ, de Haan W, Daffertshofer A, Jones BF, Manshanden I, van Cappellen van Walsum AM, *et al.* (2009): Graph theoretical analysis of magnetoencephalographic functional connectivity in Alzheimer's disease. *Brain* 132:213–224.
70. Adolphs R (2009): The social brain: Neural basis of social knowledge. *Annu Rev Psychol* 60:693–716.
71. Frith CD (2007): The social brain? *Philos Trans R Soc Lond B Biol Sci* 362:671–678.
72. Blakemore SJ (2008): The social brain in adolescence. *Nat Rev Neurosci* 9:267–277.
73. Buckner RL, Carroll DC (2007): Self-projection and the brain. *Trends Cogn Sci* 11:49–57.
74. Amodio DM, Frith CD (2006): Meeting of minds: The medial frontal cortex and social cognition. *Nat Rev Neurosci* 7:268–277.
75. Lombardo MV, Chakrabarti B, Bullmore ET, Wheelwright SJ, Sadek SA, Suckling J, Baron-Cohen S (2010): Shared neural circuits for mentalizing about the self and others. *J Cogn Neurosci* 22:1623–1635.
76. Schacter DL, Addis DR, Buckner RL (2008): Episodic simulation of future events: Concepts, data, and applications. *Ann N Y Acad Sci* 1124:39–60.
77. Ruby P, Decety J (2001): Effect of subjective perspective taking during simulation of action: A PET investigation of agency. *Nat Neurosci* 4:546–550.
78. Hassabis D, Maguire EA (2007): Deconstructing episodic memory with construction. *Trends Cogn Sci* 11:299–306.
79. Buckner RL, Andrews-Hanna JR, Schacter DL (2008): The brain's default network: Anatomy, function, and relevance to disease. *Ann N Y Acad Sci* 1124:1–38.
80. Silani G, Bird G, Brindley R, Singer T, Frith C, Frith U (2008): Levels of emotional awareness and autism: An fMRI study. *Soc Neurosci* 3:97–112.
81. Castelli F, Frith C, Happe F, Frith U (2002): Autism, Asperger syndrome and brain mechanisms for the attribution of mental states to animated shapes. *Brain* 125:1839–1849.
82. Wang AT, Lee SS, Sigman M, Dapretto M (2007): Reading affect in the face and voice: Neural correlates of interpreting communicative intent in children and adolescents with autism spectrum disorders. *Arch Gen Psychiatry* 64:698–708.
83. Kana RK, Keller TA, Cherkassky VL, Minshew NJ, Just MA (2009): Atypical frontal-posterior synchronization of theory of mind regions in autism during mental state attribution. *Soc Neurosci* 4:135–152.
84. Lombardo MV, Chakrabarti B, Bullmore ET, Sadek SA, Pasco G, Wheelwright SJ, *et al.* (2010): Atypical neural self-representation in autism. *Brain* 133:611–624.
85. Iacoboni M, Dapretto M (2006): The mirror neuron system and the consequences of its dysfunction. *Nat Rev Neurosci* 7:942–951.
86. Oberman LM, Ramachandran VS (2007): The simulating social mind: The role of the mirror neuron system and simulation in the social and communicative deficits of autism spectrum disorders. *Psychol Bull* 133:310–327.
87. Wager TD, Barrett LF, Bliss-Moreau E, Lindquist KA, Duncan S, Kober H, *et al.* (2008): The neuroimaging of emotion. In: Lewis M, Haviland-Jones JM, Barrett LF, editors. *Handbook of Emotions, 3rd ed.* New York: Guilford Press, 249–271.
88. Ochsner KN, Ray RR, Hughes B, McRae K, Cooper JC, Weber J, *et al.* (2009): Bottom-up and top-down processes in emotion generation: Common and distinct neural mechanisms. *Psychol Sci* 20:1322–1331.
89. Cunningham WA, Johnson MK, Raye CL, Chris Gatenby J, Gore JC, Banaji MR (2004): Separable neural components in the processing of black and white faces. *Psychol Sci* 15:806–813.
90. Singer T, Seymour B, O'Doherty J, Kaube H, Dolan RJ, Frith CD (2004): Empathy for pain involves the affective but not sensory components of pain. *Science* 303:1157–1162.
91. Wicker B, Keysers C, Plailly J, Royet JP, Gallese V, Rizzolatti G (2003): Both of us disgusted in my insula: The common neural basis of seeing and feeling disgust. *Neuron* 40:655–664.
92. Craig AD (2002): How do you feel? Interoception: The sense of the physiological condition of the body. *Nat Rev Neurosci* 3:655–666.
93. Critchley HD, Wiens S, Rotshtein P, Ohman A, Dolan RJ (2004): Neural systems supporting interoceptive awareness. *Nat Neurosci* 7:189–195.
94. Minshew NJ, Webb SJ, Williams DL, Dawson G (2006): Neuropsychology and neurophysiology of autism spectrum disorders. In: Moldin SO, Rubenstein JL, editors. *Understanding Autism: from Basic Neuroscience to Treatment*. Boca Raton, FL: Taylor & Francis, 379–415.
95. Di Martino A, Shehzad Z, Kelly C, Roy AK, Gee DG, Uddin LQ, *et al.* (2009): Relationship between cingulo-insular functional connectivity and autistic traits in neurotypical adults. *Am J Psychiatry* 166:891–899.
96. Hagmann P, Cammoun L, Gigandet X, Meuli R, Honey CJ, Wedeen VJ, Sporns O (2008): Mapping the structural core of human cerebral cortex. *PLoS Biol* 6:e159.
97. Buckner RL, Sepulcre J, Talukdar T, Krienen FM, Liu H, Hedden T, *et al.* (2009): Cortical hubs revealed by intrinsic functional connectivity: Mapping, assessment of stability, and relation to Alzheimer's disease. *J Neurosci* 29:1860–1873.
98. Llinas R, Ribary U, Contreras D, Pedroarena C (1998): The neuronal basis for consciousness. *Philos Trans R Soc Lond B Biol Sci* 353:1841–1849.
99. Behrens TE, Johansen-Berg H, Woolrich MW, Smith SM, Wheeler-Kingshott CA, Boulby PA, *et al.* (2003): Non-invasive mapping of connections between human thalamus and cortex using diffusion imaging. *Nat Neurosci* 6:750–757.
100. Mizuno A, Villalobos ME, Davies MM, Dahl BC, Muller RA (2006): Partially enhanced thalamocortical functional connectivity in autism. *Brain Res* 1104:160–174.
101. Nayate A, Bradshaw JL, Rinehart NJ (2005): Autism and Asperger's disorder: Are they movement disorders involving the cerebellum and/or basal ganglia? *Brain Res Bull* 67:327–334.
102. Leopold DA (2009): Neuroscience: Pre-emptive blood flow. *Nature* 457: 387–388.
103. Goldberger AL, Amaral LA, Hausdorff JM, Ivanov P, Peng CK, Stanley HE (2002): Fractal dynamics in physiology: Alterations with disease and aging. *Proc Natl Acad Sci U S A* 99(suppl 1):2466–2472.
104. Raznahan A, Toro R, Daly E, Robertson D, Murphy C, Deeley Q, *et al.* (2009): Cortical anatomy in autism spectrum disorder: An in vivo MRI study on the effect of age. *Cereb Cortex* 20:1332–1340.
105. McAlonan GM, Daly E, Kumari V, Critchley HD, van Amelsvoort T, Suckling J, *et al.* (2002): Brain anatomy and sensorimotor gating in Asperger's syndrome. *Brain* 125:1594–1606.
106. Rubenstein JL, Merzenich MM (2003): Model of autism: Increased ratio of excitation/inhibition in key neural systems. *Genes Brain Behav* 2:255–267.
107. Herbert MR, Ziegler DA, Makris N, Filipek PA, Kemper TL, Normandin JJ, *et al.* (2004): Localization of white matter volume increase in autism and developmental language disorder. *Ann Neurol* 55:530–540.